Am J Physiol Renal Physiol 319: F84–F92, 2020.
First published June 1, 2020; doi:10.1152/ajprenal.00603.2019.

RESEARCH ARTICLE | *Translational Physiology*

Pharmacokinetics and pharmacodynamics of TTI-101, a STAT3 inhibitor that blocks muscle proteolysis in rats with chronic kidney disease

Liping Zhang,[1] Ying Wang,[1] Yanlan Dong,[1] Zihong Chen,[1] Thomas K. Eckols,[2] Moses M. Kasembeli,[2] David J. Tweardy,[2,3] and William E. Mitch[1]

[1]*Nephrology Division, Department of Medicine, Baylor College of Medicine, Houston, Texas;* [2]*Division of Internal Medicine, Department of Infectious Disease, Infection Control and Employee Health, The University of Texas MD Anderson Cancer Center, Houston, Texas; and* [3]*Department of Molecular and Cellular Oncology, The University of Texas MD Anderson Cancer Center, Houston, Texas*

Submitted 29 December 2019; accepted in final form 27 May 2020

Zhang L, Wang Y, Dong Y, Chen Z, Eckols TK, Kasembeli MM, Tweardy DJ, Mitch WE. Pharmacokinetics and pharmacodynamics of TTI-101, a STAT3 inhibitor that blocks muscle proteolysis in rats with chronic kidney disease. *Am J Physiol Renal Physiol* 319: F84–F92, 2020. First published June 1, 2020; doi:10.1152/ajprenal.00603.2019.—Loss of muscle proteins increases the morbidity and mortality of patients with chronic kidney disease (CKD), and there are no reliable preventive treatments. We uncovered a STAT3/CCAAT-enhancer-binding protein-δ to myostatin signaling pathway that activates muscle protein degradation in mice with CKD or cancer; we also identified a small-molecule inhibitor of STAT3 (TTI-101) that blocks this pathway. To evaluate TTI-101 as a treatment for CKD-induced cachexia, we measured TTI-101 pharmacokinetics and pharmacodynamics in control and CKD rats that were orally administered TTI-101or its diluent. The following two groups of gavage-fed rats were studied: sham-operated control rats and CKD rats. Plasma was collected serially (0, 0.25, 0.5, 1, 2, 4, 8, and 24 h) following TTI-101 administration (at oral doses of 0, 10, 30, or 100 mg/kg). Plasma levels of TTI-101 were measured by LC-MS/MS, and pharmacokinetic results were analyzed with the PKSolver program. Plasma TTI-101 levels increased linearly with doses; the maximum plasma concentrations and time to maximal plasma levels (~1 h) were similar in sham-operated control rats and CKD rats. Notably, gavage treatment of TTI-101 for 3 days produced TTI-101 muscle levels in sham control rats and CKD rats that were not significantly different. CKD rats that received TTI-101 for 7 days had suppression of activated STAT3 and improved muscle grip strength; there also was a trend for increasing body and muscle weights. TTI-101 was tolerated at doses of 100 $mg \cdot kg^{-1} \cdot day^{-1}$ for 7 days. These results with TTI-101 in rats warrant its development as a treatment for cachexia in humans.

chronic kidney disease; inflammation; muscle wasting; skeletal muscle; STAT3

INTRODUCTION

Chronic kidney disease (CKD) is a major public health problem in the United States (15). For example, since 2001, there has been an estimated 60% increase in patients in the United States developing end-stage renal disease (6). Patients with CKD are at increased risk of developing complications of CKD, including accelerated muscle protein breakdown plus suppression of protein synthesis in muscle; these catabolic responses lead to negative muscle protein balance with protein wasting (18, 19). This is relevant because loss of muscle mass interferes with the quality of life and increases morbidity and mortality. Unfortunately, there are no reliable treatment strategies that block muscle protein losses in patients with CKD or other catabolic conditions (e.g., diabetes, cancer, and chronic inflammatory conditions).

Previously, we identified myostatin, a negative regulator of muscle growth, as an initiator of muscle protein wasting in mice with CKD or other catabolic conditions. To assess proteolytic mechanisms that could cause muscle protein loss, we examined whether a humanized anti-myostatin peptibody that inhibits myostatin function would suppress loss of muscle proteins stimulated by CKD (7, 23). Administration of the anti-myostatin peptibody to mice with CKD did block both muscle wasting and expression of the proinflammatory cytokines IL-6 and TNF-α (23). However, further development of this approach as a method of blocking muscle wasting was suspended when patients with Duchenne's muscular dystrophy participating in a phase I study supported by Acceleron Pharma and Shire Pharmaceuticals developed unexplained nose and gum bleeding during treatment with decoy myostatin receptors. This unexpected adverse outcome led the sponsors to halt the study (https://quest.mda.org/news/update-ace-031-clinical-trials-duchenne-md). Thus, development of alternative drugs that block myostatin function and muscle wasting is needed.

What stimulates myostatin expression in muscles of CKD mice? One potential stimulus is that CKD activates STAT3 in skeletal muscles. This possibility is raised because activation of STAT3 through its phosphorylation at Tyr^{705} stimulates the transcription and expression of CCAAT-enhancer-binding protein-δ (C/EBPδ). These responses have been followed by an increase in the expression of myostatin and, ultimately, muscle atrophy (22). Currently, there are no clinically available drugs that directly target STAT3 and prevent it from activating muscle wasting. However, Tweardy and colleagues initiated a program to develop a small-molecule inhibitor of STAT3 that targets the phosphotyrosyl (pY)-binding site within the SH2 domain of STAT3 (20). Their investigations identified an inhibitor of STAT3, TTI-101 (formerly C188-9) (13, 20). Characterization of TTI-101 actions revealed that it directly binds to STAT3 with high affinity (K_d = 4.7 nM) and blocks the binding of STAT3 to its pY-peptide ligand with K_i = 136 nM (20); TTI-101 does not inhibit upstream JAK or Src

Correspondence: L. Zhang (lipingz@bcm.edu).

kinases (13). Administration of TTI-101 to mice with CKD was found to block uremia-induced muscle wasting (22). The response to STAT3 inhibition in mice with CKD could extend to other conditions because STAT3 activation develops in muscle wasting conditions, including cancer (2, 4), obesity (11), and burn injury (10).

In the present experiments, we examined the pharmacokinetics (PK) and pharmacodynamics (PD) of TTI-101 in a rat model of CKD. Our goal was to determine how the accumulation of the inhibitor and STAT3 in muscle is regulated. Rats were studied because they have physiological similarities to humans, and there is greater reproducibility of CKD results and sensitivity to drugs in rats. Specifically, we administered TTI-101 by oral gavage to control and CKD rats, and we collected serial blood samples for measurement of plasma TTI-101 levels. Our experiments were directed at comparing the plasma PK of TTI-101 in normal control rats and CKD rats to determine whether the drug accumulates in skeletal muscles of rats with CKD and whether it reverses the loss of muscle protein.

MATERIALS AND METHODS

Induction of CKD in rats and treatment with TTI-101. The Baylor College of Medicine Institutional Animal Care and Use Committee approved all animal experiments and procedures. Male Sprague-Dawley rats weighing 50–75 g were obtained from Charles River Laboratories (Raleigh, NC) and housed in temperature-controlled rooms with a 12:12-h light-dark cycle. Water and food were provided ad libitum. Our model of CKD was derived by subtotal nephrectomy, as previously described (1, 12). Briefly, rats were anesthetized, and approximately two-thirds of the left renal artery was ligated (Fig. 1*A*). Subsequently, rats were given 0.45% NaCl in drinking water ad libitum and fed with 6% protein chow (TD.90016, Envigo, Teklab, Indianapolis, IN) to suppress renal hypertrophy and reduce uremia-induced mortality. After an additional week, the right kidney was removed (uninephrectomy), and 0.45% NaCl in drinking water and

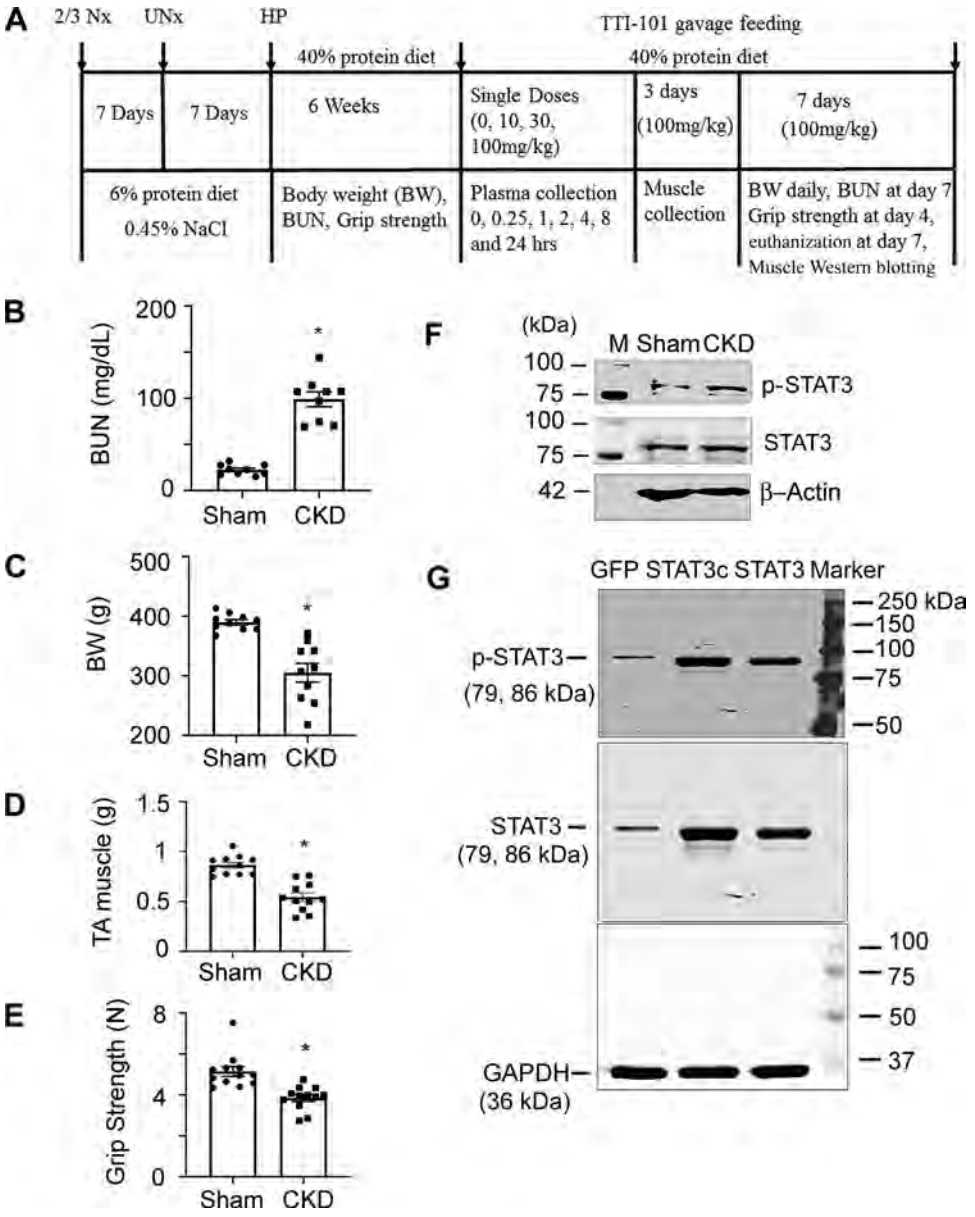

Fig. 1. Schematic and details of the chronic kidney disease (CKD) protocol and its characteristics in CKD rats versus sham control rats. *A*: details and timing of the CKD protocol and TTI-101 treatments. Rats with CKD exhibited high blood urea nitrogen (BUN) levels (*B*) and had decreases in body weight (BW; *C*) and weight of tibialis anterior (TA) muscles (*D*) as well as reduced grip strength (*E*) versus sham control rats. *F*: TA muscles of CKD rats had high expression of phosphorylated (p-)STAT3. *G*: antibodies to p-STAT3 and STAT3 were verified using lysates of C2C12 cells that were transfected with labeled plasmids. Antibodies against p-STAT3 or STAT3, which yielded bands of the correct molecular weight (79 and 86 kDa, respectively) and high level expression were found in constitutively active STAT3 (Stat3C)- or STAT3-transfected cells. Data are shown as means ± SE; $n \geq 9$ rats in each group. *$P <$ 0.05 vs. sham control rats.

the 6% protein diet were continued. One week later, rats were fed a high-protein diet (40% protein, TD 90018, Envigo, Teklab) to induce uremia and its complications (e.g., weight loss, increased levels of blood urea nitrogen, and metabolic acidosis). Rats with CKD were pair fed with sham-operated (sham) control rats (i.e., the abdomen was opened, and the kidneys were manipulated without kidney injury) (1, 12). Body weight and blood urea nitrogen of rats were measured at 2 wk after the high-protein diets were begun.

TTI-101 was formulated for oral dosing by dissolving it in a mixture of Food and Drug Administration-approved oral excipients (Labrasol: 60% and PEG-400: 40%). Briefly, 500 mg TTI-101 was mixed with 7.5 mL Labrasol followed by 1 min of sonication. Five milliliters of PEG-400 were then added to the mixture followed by 5 min of sonication. The final concentration of TTI-101 was 40 mg/mL.

For the single-dose PK experiment, sham control rats and CKD rats received TTI-101 by oral gavage at the following doses: 0, 10, 30, or 100 mg/kg. Blood was collected from the orbital venous sinuses into anticoagulant EDTA-treated tubes using heparinized capillary tubes at 0 (predose), 0.25, 0.5, 1, 2, 4, 8, and 24 h after a single dose of TTI-101. After centrifugation (2,000 *g*, 15 min at 4°C), the plasma was immediately placed in a −80°C freezer until samples were analyzed. At each time point and dose, four rats were evaluated.

In the PD experiments, sham control rats and CKD rats were given TTI-101 or vehicle by oral gavage daily. One of the groups of rats received 100 $mg \cdot kg^{-1} \cdot day^{-1}$ TT1-101 for 3 days, and rats were then euthanized with an injection of CCM Rodent Combo III from Baylor College of Medicine. Skeletal muscles were collected, immediately frozen in liquid nitrogen, and stored in a −80°C freezer until TTI-101 was measured. Another group of rats was administered TTI-101 (100 mg/kg) by oral gavage for 7 days, and body weights were monitored daily. Grip strength was measured on *day 4*, and blood urea nitrogen was measured on *day 7*. When rats were euthanized by injecting them with an overdose of CCM Rodent Combo III, tibialis anterior (TA) muscles were collected and processed for cryosections for immunostaining; alternatively, muscle samples were immediately frozen in liquid nitrogen and stored in a −80°C freezer until Western blot analysis (Fig. 1*A*).

Extraction of TTI-101 from rat plasma. TTI-101 was extracted from plasma by adding 25 μL rat plasma to 75 μL methanol containing 200 ng/mL 7-hydroxy coumarin (internal standard). This mixture was vortexed for 2–3 s and placed on ice for 5 min to denature plasma proteins. The mixture was then added to 100 μL of 0.2% formic acid containing 7-hydroxy-coumarin (200 ng/mL), and the mixture was vortexed for 2–3 s. Subsequently, the mixture was centrifuged at maximum speed (13K rpm) for 5 min at 5°C; 150 μL of clear supernatant were collected for each analysis.

Extraction of TTI-101 from rat muscles. TA muscles were placed in homogenizer tubes containing methanol at a 1:10 ratio (e.g., 100 mg of muscle placed in 1 mL of methanol), and stainless steel homogenizing beads were added. Muscles were homogenized using an Omni Tissue Homogenizer (Kennesaw, GA); the homogenate was centrifuged, and 50 μL of solvent were then removed and added to 50 μL of 0.2% formic acid containing 7-hydroxy-coumarin (200 ng/mL). The mixture was transferred to a LC sample vial and used to measure TTI-101.

PK analyses of TTI-101 in rat plasma and muscle samples. Levels of TTI-101 were measured in extracts of rat plasma and muscles in conjunction with the Pharmaceutical Science Facility of the Institute for Applied Cancer Science, University of Texas MD Anderson Cancer Center (Houston, TX). A Waters Xevo TQ-S mass spectrometer with Waters Acquity UPLC with temperature-controlled autosampler was used for the assay. Chromatographic separation was achieved using a Waters Acquity BEH C18 1.7 μm 2 × 100-mm column at a temperature of 60°C. The aqueous mobile phase (*solvent A*) was created as follows: 0.1% (vol/vol) formic acid in diH_2O. The organic phase (*solvent B*) was 0.1% formic acid in 80:20 acetonitrile-methanol.

Mass spectrometry was performed in positive ion mode using multiple reaction monitoring transition pairs m/z 494.13 > 322.02 for TTI-101 and 167.0 > 107 for 7-hydroxy-coumarin. Optimal signals were obtained with a clone voltage setting of 50 V for TTI-101 and 20 V for 7-hydroxy-coumarin. Collision energy was 23 eV and 21 eV for TTI-101 and 20 V for 7-hydroxy-coumarin, respectively.

The PKSolver add-in program for PK and PD data analyses in Microsoft Excel was used for data analysis (26). The noncompartmental analysis model was applied.

Grip strength measurement. Grip strength was measured daily for 2 consecutive days using a grip strength meter (Columbus Instruments). Each day, five grip strengths at 1-min intervals were assessed, and the average grip strength over 2 days was calculated (22).

Western blot analysis. Rat skeletal muscle mixed fibers [i.e., TA muscle] were homogenized in RIPA buffer plus phosphatase inhibitor and Complete Mini Protease inhibitors (Roche). Muscle lysates were processed for Western blot analysis to evaluate proteins using antibodies against phosphorylated (p-)STAT3 (Tyr^{705} D3A7, no. 9145, 1:1,000 dilution) and STAT3 (124H6, no. 9139, 1:1,000) from Cell Signaling Technology (Beverly, MA) (21, 23). Anti-GAPDH (MAB374, 1:500 dilution) or anti-β-actin (SAB4301137, 1:1,000) from Sigma-Aldrich (Burlington, MA) was used to detect proteins as a loading control. To validate antibodies of p-STAT3 and STAT3, we transfected C2C12 cells with plasmids expressing constitutively active STAT3 or wild-type STAT3 for 24 h. Green fluorescent protein-transfected cells were used as a control, and cell lysates were processed for Western blot analysis with anti-p-STAT3 or STAT3. The molecular weights (79 and 86 kDa) and levels of STAT3 confirmed the accuracy of the antibodies (Fig. 1*G*).

RT-PCR analyses. RNA was extracted from TA muscles using an RNA extraction kit (Qiagen), and cDNA was prepared using the iScript cDNA synthesis kit (Bio-Rad). Duplicate PCRs were performed using SYBR green (Bio-Rad) on a Bio-Rad CFX96 real-time thermal cycle (21, 24). Relative gene expression in muscles was calculated from threshold cycle (C_t) values using GAPDH as an internal control [relative expression = $2^{(\text{sample } C_t - \text{GAPDH } C_t)}$] (24, 25). The sequences of the primers used were as follows: 5′-CTCCAGAATAGAAGCCATA-3′ (forward) and 5′-GCAGAAGTTGTCTTATAGC-3′ (reverse) for myostatin (NM_019151.1), 5′-TAGTGTGCTATGCCTAAG-3′ (forward) and 5′-TATTGCCAGTTCTTCGTA-3′ (reverse) for IL-6 (NM_012589.2), and 5′-CATTCTTCCACCTTTGAT-3′ (forward) and 5′-CTGTAGCCATATTCATTGT-3′ (reverse) for GAPDH (NM_017008.4).

Immunostaining and myofiber area measurements. Myofiber sizes were measured from cryo-cross sections of TA muscles that were immunostained with anti-laminin (L9303, Sigma-Aldrich, 1:30 dilution,). Briefly, cross sections of TA muscles were fixed in 4% paraformaldehyde and permeabilized by incubating samples in 0.3% Triton X-100 in PBS followed by blocking with "Protein Block" (DAKO, Carpinteria, CA) for 1 h at room temperature. Sections were then incubated with anti-laminin that was mixed in "Antibody Dilute" (DAKO) overnight at 4°C followed by detection of primary antibodies using secondary antibodies that were conjugated to Alexa Fluor 568 (Invitrogen). Tissues were visualized using Nikon 80i microscope, and images were acquired using a Digital Sight-cooled camera, and NIS Elements Br 3.0 software (Melville, NY) was used to measure myofiber area.

Statistical analysis. Results are expressed as means ± SE. Significance testing was performed using a Student's *t* test when results from two groups were compared; two-way ANOVA followup with Kruskal-Wallis was used when data from three or more groups were studied. Statistical significance was set at $P < 0.05$. GraphPad Prism8 was used for analysis and figure plotting.

RESULTS

TT1-101 administration to a rat model of CKD created by subtotal nephrectomy. CKD was created by subtotal nephrectomy. Nephrectomized rats were initially fed a 6% protein diet to improve recovery from surgery and suppress renal hypertrophy (Fig. 1*A*). One week after the second subtotal nephrectomy, rats were fed a high-protein diet to induce uremia. After 2 wk of high-protein diet feeding, average blood urea nitrogen was three- to four-fold higher in subtotal nephrectomy rats versus pair-fed sham control rats (Fig. 1*B*), and they developed a significant ($P < 0.05$) decrease in whole body as well as TA muscle weights ($P < 0.05$; Fig. 1, *C* and *D*). In addition, grip strength was decreased versus values from sham control rats ($P < 0.05$; Fig. 1*E*). As we have previously reported in mice, CKD stimulates STAT3 levels in TA muscles of CKD rats, and the difference was detected by Western blot analysis using antibodies against p-STAT3 and STAT3 (Fig. 1*F*). These antibodies were validated by Western blot analysis based on molecular weight and protein levels in cells with gene overexpression (see MATERIALS AND METHODS and Fig. 1*G*). We evaluated TA muscles mainly because p-STAT3 is detected in different types of CKD mouse muscle fibers, including red fiber muscles (soleus) and white fiber muscles (extensor digitorum longus) as well as in mixed-fiber muscles (gastrocnemius and TA muscles). To eliminate concerns about the two types of muscle fiber giving different results, we show results in mixed-fiber TA muscles in all experiments.

After 6 wk of high-protein diet feeding, sham control rats and CKD rats each received a single dose of TTI-101 by oral gavage. Plasma was collected at different times following oral gavage, and samples were stored at −80°C for measurement of TTI-101. Rats were euthanized after the final blood collection.

Optimization of sample preparation for measurement of TTI-101. The lower limit of quantification of TTI-101 (*m/z* 494 → 322) in standard was established as 50 ng/mL with a coefficient of variation of 0.75, which is well above the "noise" level. No interfering peaks were observed at the expected retention time of 2.4 ± 0.02 min (Fig. 2*A*). The calibration curve for TTI-101 was constructed from the peak area ratio of TTI-101 to its internal standard (7-hydroxy-coumarin) using the least-squares quadratic regression analysis with $1/x^2$ weighting. $R^2 \geq 0.99$ and the calibration range was 50–20 μg/mL (Fig. 2*B*). Selectivity of the extraction process was established for rat plasma samples in two separate studies. For each study, five standards of TTI-101 were included and calibrated. To begin the process of determining whether levels of TTI-101 could be measured in rat plasma, we performed a preliminary study: sham control rats were administered TTI-101 by oral gavage of doses (0, 10, 30, or 100 mg/kg once), and plasma was collected 4 h later for measurement of TTI-101, as described above. We found that the analyte area corresponding to TTI-101 (Fig. 2*C*) was higher when increasing doses of TTI-101 were administered.

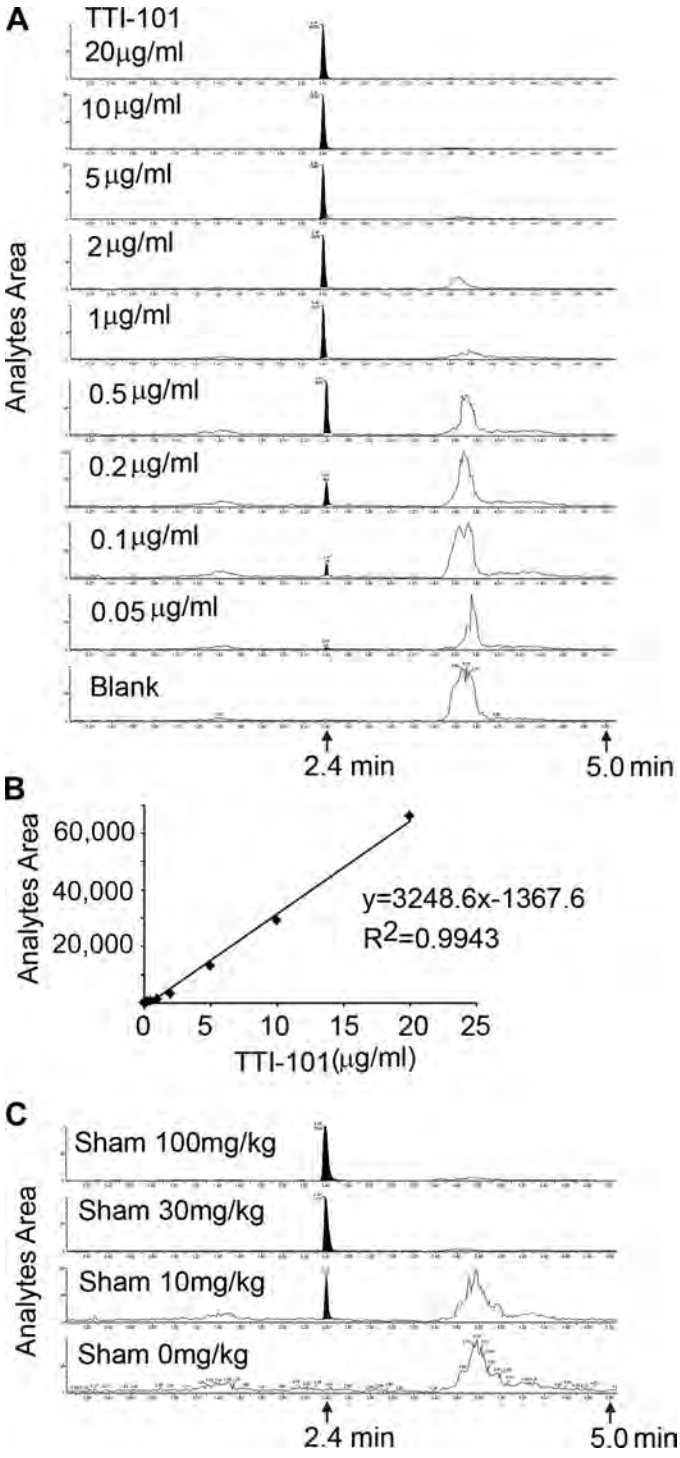

Fig. 2. Measurement of TTI-101 in plasma by LC-MS/MS. *A* and *B*: the location of the TTI-101 peak (*A*) as well as correlation of the area under the curve and amounts of TTI-101 analyzed (*B*). *C*: LC-MS/MS of plasma TTI-101 in response to dose of gavage feeding to sham control rats.

PK of TTI-101 in sham control rats and CKD rats. We proceeded by performing plasma TTI-101 PK analysis based on measuring TTI-101 levels in plasma samples that were serially obtained from sham control rats and CKD rats following administration of TTI-101 at three dose levels (10, 30, and 100 mg/kg) by oral gavage (Fig. 3). In sham control rats, TTI-101 was detected in the plasma within 15 min of administration of each dose and remained detectable at 24 h (Fig. 3*A*). PK analysis of plasma levels, performed using the PK-Solver program (26), demonstrated that TTI-101 reached a maximum plasma concentration at ~1 h following each dose administered (Fig. 3*A* and Table 1). We note that the half-life of TTI-101 at 10 mg/kg appears to be spuriously long (~26 h)

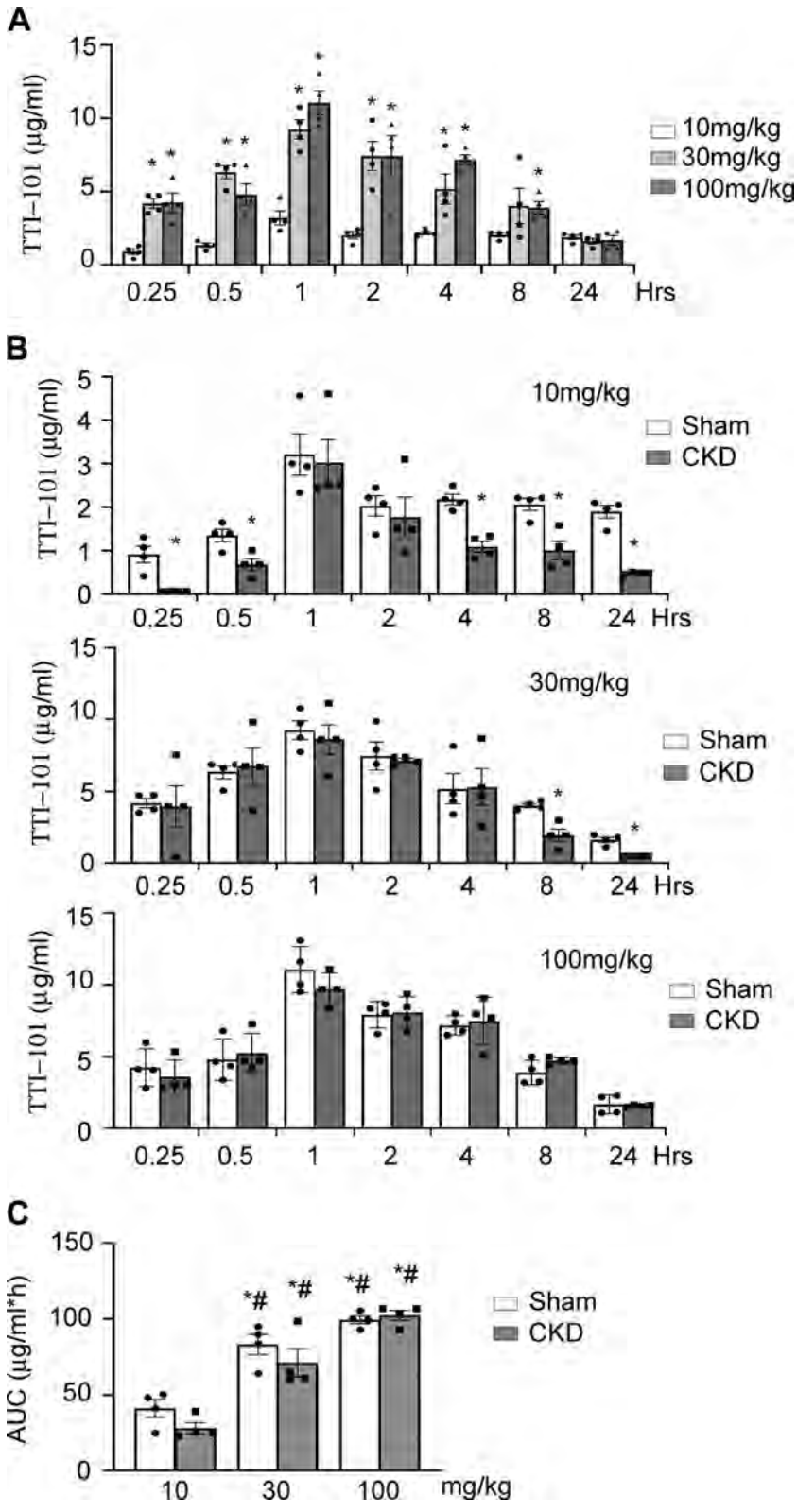

Fig. 3. Single-dose pharmacokinetics of TTI-101. After single-dose gavage feeding rats with different doses of TTI-101 (10, 30, or 100 mg/kg), the plasma was collected at different times and TTI-101 was measured. *A*: levels of TTI-101 in plasma of sham control rats that were fed with 30 or 100 mg/kg doses were significantly higher versus rats fed with 10 mg/kg TTI-101 within 8 h. *B*: plasma TTI-101 concentrations in sham control rats were similar to those in rats with chronic kidney disease (CKD) at gavage feeding doses of 30 or 100 mg/kg. *C*: mean area under the plasma drug concentration-time curve up to *time t* (AUC_{0-t}) of TTI-101 from plasma of rats fed with 30 or 100 mg/kg was significantly higher versus that of rats fed with 10 mg/kg. There was no significant difference between sham control rats and CKD rats at any dose. Data are shown as means ± SE; $n = 4$ rats in each group. *$P < 0.05$ vs. sham control rats treated with 10 mg/kg TTI-101; #$P < 0.05$ vs. CKD rats treated with 10 mg/kg TTI-101.

compared with doses at 30 and 100 mg/kg (9.4 and 8.2 h, respectively); this abnormality is most likely due to increased variability of samples at the lower limit of detection of LC-MS/MS analyses. A linear relationship was found between dose and the area under the plasma drug concentration-time curve up to *time t* (AUC_{0-t}) of TTI-101 in sham control mice (Fig. 3*C*).

In rats with CKD, TTI-101 levels were also detected in plasma at 15 min after oral administration; the TTI-101 level remained detectable at 24 h. We found that the half-life (6.2

Table 1. *Pharmacokinetic parameters of TTI-101 after oral administration*

	Maximum Plasma Concentration, μg/mL	Statistical Significance	Time to Maximal Plasma Levels, h	Half-Time, h
10 mg/kg TTI-101				
Sham	3.21 ± 0.48		1 ± 0.3	25.98 ± 1.04
CKD	3.02 ± 0.53		2.87 ± 0.79	32.08 ± 1.36
30 mg/kg TTI-101				
Sham	9.23 ± 0.66	$P < 0.05$	0.65 ± 0.14	9.42 ± 0.03
CKD	8.59 ± 1.03	$P < 0.05$	0.91 ± 0.26	6.15 ± 0.03
100 mg/kg TTI-101				
Sham	11.05 ± 0.81	$P < 0.05$	1 ± 0.2	8.2 ± 0.38
CKD	9.71 ± 0.56	$P < 0.05$	0.9 ± 0.1	10.02 ± 2.4

Data are expressed as means ± SE. TTI-101 was single-dose gavage fed to rats. TTI-101 in plasma was measured, and pharmacokinetics were analyzed using the PKSolver program. For maximum plasma concentrations, statistical comparison with sham control rats at 10 mg/kg TTI-101 was done using a Student's *t* test at a significance level of $P < 0.05$.

and 10 h, respectively; Table 1 and Fig. 3*B*) and plasma levels of TTI-101 at doses 30 and 100 mg/kg were similar to results from sham control rats. These data indicate that CKD does not alter TTI-101 elimination. Similar to results from sham control rats, we found that there was a linear relationship between dose and AUC_{0-t} of TTI-101 (Fig. 3*C*). Thus, in both sham control rats and CKD rats, oral administration of TTI-101 provides similar plasma PK results, including plasma half-lives and drug exposures.

TTI-101 administration suppresses p-STAT3 in muscle and improves muscle growth in rats with CKD. To examine whether TTI-101 accumulates within skeletal muscles of sham control rats or CKD rats, we studied rats that had received either diluent or TTI-101 (100 mg/kg) by oral gavage for 3 days. There was no detectable TTI-101 in muscles of rats from either group that only received the diluent (Fig. 4*A*). In contrast, levels of TTI-101 were readily detected in muscles of rats that received TTI-101; however, there was no significant differences in TTI-101 per milligram of muscle between rats with CKD versus sham control rats (Fig. 4*B*). Treatment of TTI-101 (100 mg/kg) for 7 days was found to decrease p-STAT3 levels in muscles of rats with CKD (Fig. 4*C*). There also were decreased levels of mRNA for the proinflammatory cytokine IL-6 as well as myostatin compared with diluent-treated rats with CKD (Fig. 4, *D* and *E*). Following 7 days of TTI-101 treatment (100 mg/mL), CKD rats exhibited a trend toward increased body weight and muscle mass, but these values did not reach a level of statistical significance (Fig. 4, *F* and *G*). Consistent with this change in muscle mass, we found that grip strength and myofiber sizes were higher in CKD rats treated with TTI-101 versus CKD rats treated with diluent (Fig. 4, *H* and *I*). These results indicate that TTI-101 accumulates in the skeletal muscles of both sham control rats and CKD rats, where, in the case of CKD rats, it reduces levels of p-STAT3 and increases myofiber size and grip strength.

For toxicity evaluations, we found no detectable toxicity in rats, even at daily doses as high as 100 mg/kg for 7 days. We recognize that our model limits specific identification of TTI-101-mediated changes of function in the kidney, heart, cardiovascular, bone, and liver, because CKD is a catabolic condition that by itself interferes with different functions of each of these organs. Of note, however, we performed extensive in vitro and in vivo studies to evaluate TTI-101 for both adverse off-target and adverse on-target effects and observed no evidence of toxicity in animals or patients (3) (A. M. Tsimberidou, A. Kaseb, and D. J. Tweardy, unpublished observations). These studies include toxicokinetic studies performed successfully to obtain Federal Drug Administration approval for clinical testing of TTI-101 in patients with cancer. The results of these studies demonstrated no drug-related clinical, gross anatomic, histological, or laboratory abnormalities in rats or dogs when administered daily for 28 days up to a dose of 200 or 100 $mg \cdot kg^{-1} \cdot day^{-1}$, respectively (3) (T. K. Eckols and D.J. Tweardy, unpublished observations).

DISCUSSION

Previously, we reported that CKD stimulates loss of skeletal muscle mass through a mechanism that includes activation of STAT3 (22). In fact, the activation of STAT3 increases the levels of the transcriptional factor C/EBPδ, and this leads to upregulation of myostatin, a trigger for muscle wasting (22, 23). Similarly, we found that STAT3 activation stimulates caspase-3 activity in muscles of mice with cancer cachexia. This is relevant because activated caspase-3 promotes the ubiquitin-proteasome system, resulting in an acceleration of muscle protein degradation (8, 16). In addition, STAT3 also is activated in muscle wasting conditions, including cancer (4, 5), obesity (11), and burn injury (10). It is possible, therefore, that targeting STAT3 activity might prevent muscle wasting in catabolic conditions besides CKD. Previously, we uncovered that TTI-101 exhibits promise for the development of a drug that can be administered safely and effectively to treat or prevent cachexia (16, 22). In the present report, we performed PK and PD analyses of TTI-101 administered by oral gavage in a rat model of CKD. The results could be used in the preparation for TTI-101 submission to the Federal Drug Administration for an Investigational New Drug application to other models of muscle wasting, such as evaluation of patients treated by hemodialysis. In the present analysis, rats were studied because they have physiological similarities to humans. Only male rats were examined, as female rats are less prone to proteinuria (9). In contrast, women not only are more likely to develop CKD than men but also have poorer outcomes (14). Therefore, our inhibitor should be effective for both men and women. Specifically, we formulated TTI-101 at a high concentration (40 mg/mL) using two Federal Drug Administration-approved oral excipients that would allow administration to rats by oral gavage, a key step on the path toward developing TTI-101 for oral administration to patients with CKD. The

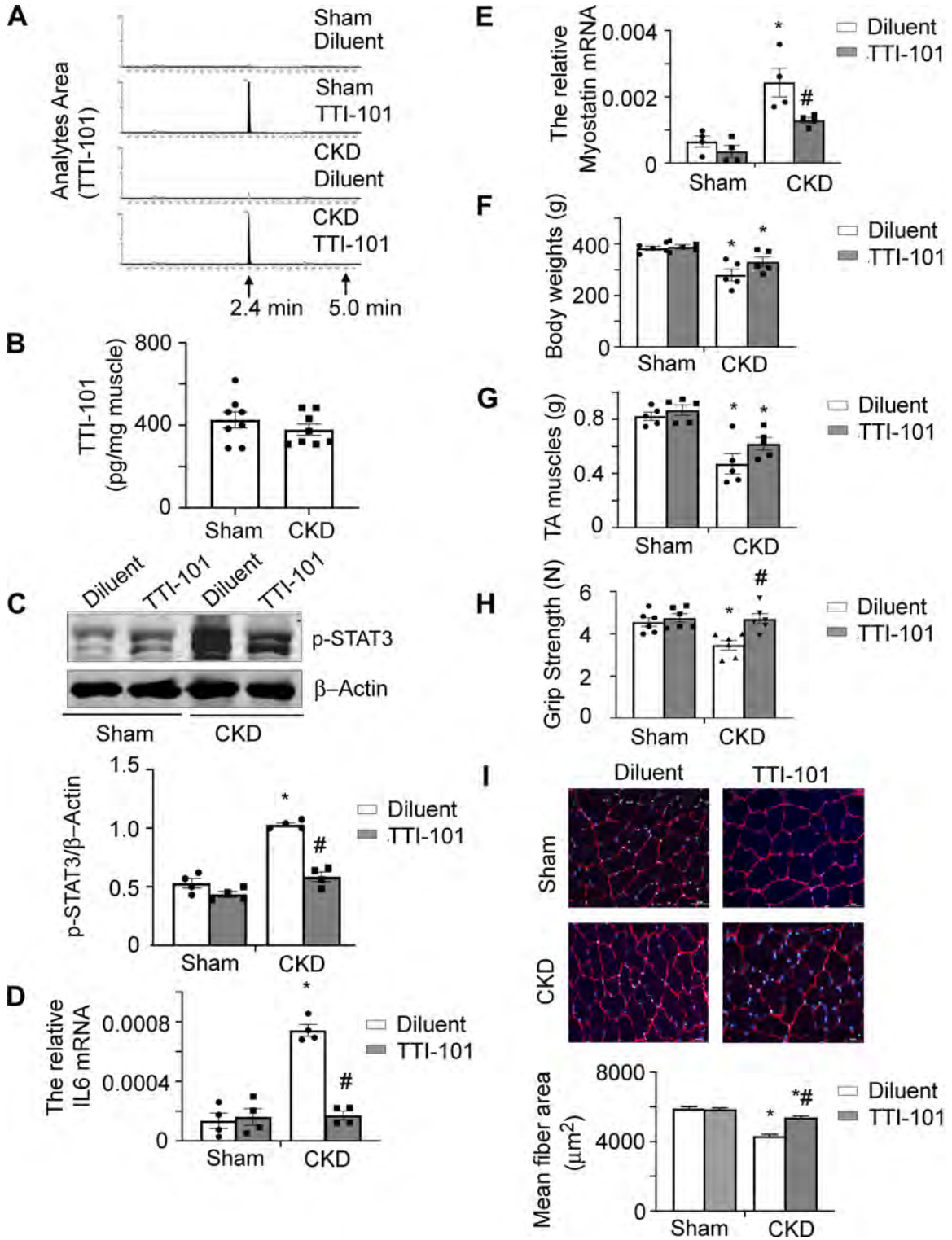

Fig. 4. Administration of TTI-101 decreased levels of phosphorylated (p-)STAT3 in muscles of chronic kidney disease (CKD) rats and tended to increase body and muscle weights. *A*: 3 days after gavage feeding TTI-101 (100 mg/kg) to rats caused its accumulation in muscle. *B*: TTI-101 levels (μg) in muscle were calculated based *A* as per milligram of muscle from sham control and CKD rats. There was no significant difference between sham control and CKD rats. *C*−*I*: TTI-101 was gavage fed to rats daily for 7 days. CKD-induced p-STAT3 in muscle was suppressed (*C*). Inhibitor also inhibited IL-6 (*D*) and myostatin (*E*) mRNA in muscles of CKD rats. The inhibitor tend to improve body weight (*F*) and tibialis anterior (TA) muscle weight (*G*). It also increased the grip strength of CKD rats (*H*). *I*: cross-sections of TA muscle were immunostained with anti-laminin (*top*). The myofiber area was measured, and average myofiber size is shown with standard errors (*bottom*). TTI-101 improved myofiber size in muscles of CKD rats. $n \geq 4$. *$P < 0.05$ vs. sham control rats treated with diluent; #$P < 0.05$ vs. CKD rats treated with diluent.

results of our assessment of the measurement of TTI-101 were of special interest because we used LC-MS/MS methodology to measure plasma and skeletal muscle levels of TTI-10. Our results demonstrated that plasma levels of TTI-101 increase linearly with dose, and the maximum plasma concentrations of TTI-101 and time to maximal plasma levels (1 h) were predictably similar between rats in the sham control and CKD groups. Of note, TTI-101 administration to rats was not accompanied by the development of any adverse effects, even at doses as high as 100 $mg \cdot kg^{-1} \cdot day^{-1}$ for 7 days. Specifically, body and muscle weights of TTI-101-treated CKD rats tended to increase compared with diluent-treated CKD rats.

Notably, we found decreased expression of p-STAT3 along with decreased levels of myostatin and IL-6 mRNA in CKD rats treated with TTI-101. The treatment response to TTI-101 suggests that the drug can inhibit inflammation in skeletal muscles, and this conclusion is consistent with our earlier reports. In those experiments, we found that STAT3 activation can induce expression of the transcription factor of C/EBPδ, which, in turn, increases myostatin expression and stimulates the expression of IL-6 (22, 25). Inhibition of the activity of STAT3 also improved myofiber size and grip strength in rats with CKD. These responses are consistent with a report (17) showing that myofiber hypertrophy is closely related to improvements in grip strength of mice with myopathy. As far as we know, we are the first group to define PK parameters obtained using an inhibitor of STAT3 in vivo. Interestingly, there are similarities among results we obtained in control and CKD rats versus those we obtained from studies in mice (22). Specifically, treatment of CKD rats with TTI-101 actually increased body and muscle weights of CKD rat but were not statistically different. Possibly, the lack of a statistical difference may have reflected a short time of analysis. This possibility is suggested because we have previously treated mice with CKD for a longer period of time and determined that TTI-101 can suppress CKD-induced muscle wasting (22). We have also administered TTI-101 to wild-type rats or dogs daily for 28 days and at doses of 200 $mg \cdot kg^{-1} \cdot day^{-1}$ or 100 $mg \cdot kg^{-1} \cdot day^{-1}$, respectively. Under those conditions, we found no drug-related or clinical, gross anatomic, histological, or laboratory abnormalities in rats or dogs (3). In addition, TTI-101 concentrates three- to sixfold in tissue, leading to reduced levels of activated STAT3 (p-STAT3) (3). In the present study, each of the three doses of TTI-101 administered to rats with CKD was associated with the appearance of TTI-101 in plasma within 15 min. Moreover, the concentration of TTI-101 reached a maximum plasma level within 1 h. The present results indicate that dosing of TTI-101 in 60% Labrasol and 40% PEG-400 followed by sonication was successful in dissolving TTI-10, making TTI-101 more bioavailable than its administration as a suspension. We conclude that TTI-101 has the potential to develop into an orally bioavailable drug to treat CKD or other catabolic diseases in patients to improve muscle quality.

GRANTS

This work was supported by National Institutes of Health Grants R01DK37175 (to W. E. Mitch), R42DK10449401A1 (to D. J. Tweardy), and R01HL147108 (to P. I. X. Wehrens, L. Zhang, Co-Investigator). We also acknowledge the generous support of Dr. and Mrs. Harold Selzman. L. Zhang was supported by a Norman S. Coplon extramural research grant from Satellite Health, by American Diabetic Association Grant 1-11-BS-194, and by a pilot/feasibility award from the Diabetes Research Center (P30DK079638).

DISCLOSURES

D.J. Tweardy is a co-founder of Tvardi. All other authors certify they have no conflicts of interest, financial or otherwise.

AUTHOR CONTRIBUTIONS

L.Z., T.K.E., D.J.T., and W.E.M. conceived and designed research; L.Z., Y.W., Y.D., and Z.C. performed experiments; L.Z. and Y.D. analyzed data; L.Z., M.M.K., and W.E.M. interpreted results of experiments; L.Z. prepared figures; L.Z. drafted manuscript; L.Z., M.M.K., D.J.T., and W.E.M. edited and revised manuscript; L.Z. approved final version of manuscript.

REFERENCES

1. **Bailey JL, Zheng B, Hu Z, Price SR, Mitch WE.** Chronic kidney disease causes defects in signaling through the insulin receptor substrate/phosphatidylinositol 3-kinase/Akt pathway: implications for muscle atrophy. *J Am Soc Nephrol* 17: 1388–1394, 2006. doi:10.1681/ASN.2004100842.
2. **Baltgalvis KA, Berger FG, Peña MM, Davis JM, White JP, Carson JA.** Muscle wasting and interleukin-6-induced atrogin-I expression in the cachectic $Apc^{Min/+}$ mouse. *Pflügers Arch* 457: 989–1001, 2009. doi:10.1007/s00424-008-0574-6.
3. **Bharadwaj U, Eckols TK, Xu X, Kasembeli MM, Chen Y, Adachi M, Song Y, Mo Q, Lai SY, Tweardy DJ.** Small-molecule inhibition of STAT3 in radioresistant head and neck squamous cell carcinoma. *Oncotarget* 7: 26307–26330, 2016. doi:10.18632/oncotarget.8368.
4. **Bonetto A, Aydogdu T, Jin X, Zhang Z, Zhan R, Puzis L, Koniaris LG, Zimmers TA.** JAK/STAT3 pathway inhibition blocks skeletal muscle wasting downstream of IL-6 and in experimental cancer cachexia. *Am J Physiol Endocrinol Metab* 303: E410–E421, 2012. doi:10.1152/ajpendo.00039.2012.
5. **Bonetto A, Aydogdu T, Kunzevitzky N, Guttridge DC, Khuri S, Koniaris LG, Zimmers TA.** STAT3 activation in skeletal muscle links muscle wasting and the acute phase response in cancer cachexia. *PLoS One* 6: e22538, 2011. doi:10.1371/journal.pone.0022538.
6. **Collins AJ, Kasiske B, Herzog C, Chen SC, Everson S, Constantini E, Grimm R, McBean M, Xue J, Chavers B, Matas A, Manning W, Louis T, Pan W, Liu J, Li S, Roberts T, Dalleska F, Snyder J, Ebben J, Frazier E, Sheets D, Johnson R, Li S, Dunning S, Berrini D, Guo H, Solid C, Arko C, Daniels F, Wang X, Forrest B, Gilbertson D, St Peter W, Frederick P, Eggers P, Agodoa L.** Excerpts from the United States Renal Data System 2003 Annual Data Report: atlas of end-stage renal disease in the United States. *Am J Kidney Dis* 42, *Suppl* 5: A5–A7, 2003. doi:10.1053/j.ajkd.2003.10.001.
7. **Dong J, Dong Y, Dong Y, Chen F, Mitch WE, Zhang L.** Inhibition of myostatin in mice improves insulin sensitivity via irisin-mediated cross talk between muscle and adipose tissues. *Int J Obes* 40: 434–442, 2016. doi:10.1038/ijo.2015.200.
8. **Du J, Wang X, Miereles C, Bailey JL, Debigare R, Zheng B, Price SR, Mitch WE.** Activation of caspase-3 is an initial step triggering accelerated muscle proteolysis in catabolic conditions. *J Clin Invest* 113: 115–123, 2004. doi:10.1172/JCI18330.
9. **Fanelli C, Dellê H, Cavaglieri RC, Dominguez WV, Noronha IL.** Gender differences in the progression of experimental chronic kidney disease induced by chronic nitric oxide inhibition. *BioMed Res Int* 2017: 2159739, 2017. doi:10.1155/2017/2159739.
10. **Jeschke MG, Chinkes DL, Finnerty CC, Kulp G, Suman OE, Norbury WB, Branski LK, Gauglitz GG, Mlcak RP, Herndon DN.** Pathophysiologic response to severe burn injury. *Ann Surg* 248: 387–401, 2008. doi:10.1097/SLA.0b013e3181856241.
11. **Klover PJ, Clementi AH, Mooney RA.** Interleukin-6 depletion selectively improves hepatic insulin action in obesity. *Endocrinology* 146: 3417–3427, 2005. doi:10.1210/en.2004-1468.
12. **May RC, Kelly RA, Mitch WE.** Metabolic acidosis stimulates protein degradation in rat muscle by a glucocorticoid-dependent mechanism. *J Clin Invest* 77: 614–621, 1986. doi:10.1172/JCI112344.
13. **Redell MS, Ruiz MJ, Alonzo TA, Gerbing RB, Tweardy DJ.** Stat3 signaling in acute myeloid leukemia: ligand-dependent and -independent activation and induction of apoptosis by a novel small-molecule Stat3 inhibitor. *Blood* 117: 5701–5709, 2011. doi:10.1182/blood-2010-04-280123.

14. **Savic L, Mrdovic I, Asanin M, Stankovic S, Krljanac G, Lasica R.** Gender differences in the prognostic impact of chronic kidney disease in patients with left ventricular systolic dysfunction following ST elevation myocardial infarction treated with primary percutaneous coronary intervention. *Hellenic J Cardiol* 57: 109–115, 2016. doi:10.1016/j.hjc.2015.11.001.
15. **Schoolwerth AC, Engelgau MM, Hostetter TH, Rufo KH, Chianchiano D, McClellan WM, Warnock DG, Vinicor F.** Chronic kidney disease: a public health problem that needs a public health action plan. *Prev Chronic Dis* 3: A57, 2006.
16. **Silva KA, Dong J, Dong Y, Dong Y, Schor N, Tweardy DJ, Zhang L, Mitch WE.** Inhibition of Stat3 activation suppresses caspase-3 and the ubiquitin-proteasome system, leading to preservation of muscle mass in cancer cachexia. *J Biol Chem* 290: 11177–11187, 2015. doi:10.1074/jbc.M115.641514.
17. **Tinklenberg JA, Siebers EM, Beatka MJ, Meng H, Yang L, Zhang Z, Ross JA, Ochala J, Morris C, Owens JM, Laing NG, Nowak KJ, Lawlor MW.** Myostatin inhibition using mRK35 produces skeletal muscle growth and tubular aggregate formation in wild type and TgACTA1D286G nemaline myopathy mice. *Hum Mol Genet* 27: 638–648, 2018. doi:10.1093/hmg/ddx431.
18. **Wang XH, Mitch WE.** Mechanisms of muscle wasting in chronic kidney disease. *Nat Rev Nephrol* 10: 504–516, 2014. doi:10.1038/nrneph.2014.112.
19. **Workeneh BT, Mitch WE.** Review of muscle wasting associated with chronic kidney disease. *Am J Clin Nutr* 91: 1128S–1132S, 2010. doi:10.3945/ajcn.2010.28608B.
20. **Xu X, Kasembeli MM, Jiang X, Tweardy BJ, Tweardy DJ.** Chemical probes that competitively and selectively inhibit Stat3 activation. *PLoS One* 4: e4783, 2009. doi:10.1371/journal.pone.0004783.
21. **Zhang L, Du J, Hu Z, Han G, Delafontaine P, Garcia G, Mitch WE.** IL-6 and serum amyloid A synergy mediates angiotensin II-induced muscle wasting. *J Am Soc Nephrol* 20: 604–612, 2009. doi:10.1681/ASN.2008060628.
22. **Zhang L, Pan J, Dong Y, Tweardy DJ, Dong Y, Garibotto G, Mitch WE.** Stat3 activation links a C/EBPδ to myostatin pathway to stimulate loss of muscle mass. *Cell Metab* 18: 368–379, 2013. doi:10.1016/j.cmet.2013.07.012.
23. **Zhang L, Rajan V, Lin E, Hu Z, Han HQ, Zhou X, Song Y, Min H, Wang X, Du J, Mitch WE.** Pharmacological inhibition of myostatin suppresses systemic inflammation and muscle atrophy in mice with chronic kidney disease. *FASEB J* 25: 1653–1663, 2011. doi:10.1096/fj.10-176917.
24. **Zhang L, Ran L, Garcia GE, Wang XH, Han S, Du J, Mitch WE.** Chemokine CXCL16 regulates neutrophil and macrophage infiltration into injured muscle, promoting muscle regeneration. *Am J Pathol* 175: 2518–2527, 2009. doi:10.2353/ajpath.2009.090275.
25. **Zhang L, Wang XH, Wang H, Du J, Mitch WE.** Satellite cell dysfunction and impaired IGF-1 signaling cause CKD-induced muscle atrophy. *J Am Soc Nephrol* 21: 419–427, 2010. doi:10.1681/ASN.2009060571.
26. **Zhang Y, Huo M, Zhou J, Xie S.** PKSolver: An add-in program for pharmacokinetic and pharmacodynamic data analysis in Microsoft Excel. *Comput Methods Programs Biomed* 99: 306–314, 2010. doi:10.1016/j.cmpb.2010.01.007.